

THESIS FOR THE DEGREE OF LICENTIATE OF ENGINEERING

HBV frequency multiplier 2D arrays and application

Robin Dahlbäck

Terahertz and Millimetre Wave Laboratory
Department of Microtechnology and Nanoscience (MC2)
CHALMERS UNIVERSITY OF TECHNOLOGY
Göteborg, Sweden, 2014

HBV frequency multiplier 2D arrays and application

Robin Dahlbäck

© Robin Dahlbäck, 2014

Technical Report MC2-277

ISSN 1652-0769

Department of Microtechnology and Nanoscience - MC2

Chalmers University of Technology

SE-412 96 Göteborg

Sweden

Phone: +46 (0) 31 772 1000

Front cover illustration: A conceptual rendering of a two cascaded 2D grid array frequency multipliers. The first one is a HBV based frequency tripler while the second is a polarisation separated Schottky diode based doubler.

Printed by TeknologTryck, Göteborg

Göteborg, Sweden, May, 2014

HBV frequency multiplier 2D arrays and application

Robin Dahlbäck
Terahertz and Millimetre Wave Laboratory
Department of Microtechnology and Nanoscience - MC2
Chalmers University of Technology
SE-412 96 Göteborg
Sweden

Abstract

The utilisation of the THz spectrum (0.3-3 THz) is hampered by technological difficulties to generate power at these frequencies. Applications within diverse fields such as radio astronomy, security imaging, life sciences, high data rate communications and production monitoring could benefit significantly from compact, high power THz signal sources operating at room temperature. This thesis reports on the design and fabrication aspects of varactor diode based 2D array frequency multipliers. Both free space operating and waveguide enclosed Heterostructure Barrier Varactors (HBVs) arrays are discussed in detail. The goal of this work has been to design, fabricate and characterise high power varactor 2D array frequency multipliers, enabling increased power handling capabilities and output power of future THz frequency multipliers. This approach is expected to offer excellent frequency and power scalability for THz signal sources.

An altogether waveguide integrated 249 GHz HBV 2D array frequency tripler is presented together with measurement data. With an output power of 18 mW at 248 GHz and a conversion efficiency of 2 %, this is the highest frequency of operation and output power reported to date for waveguide enclosed 2D array frequency multipliers.

A 346 GHz imaging system is also presented as an application example for powerful THz signal sources. The system uses an imaging algorithm based on the Born approximation and produces images with a voxel size of $0.1 \times 0.1 \text{ mm}^2$ (approximately 1/10 of the free space wavelength).

Keywords: THz, 2D array frequency multipliers , Heterostructure Barrier Varactors (HBVs), varactor frequency multipliers, terahertz sources, sub-millimetre waves, THz imaging

List of papers

This thesis is based on the following appended papers:

- [A] **R. Dahlbäck**, J. Vukusic, R.M. Weikle II, and J. Stake, "A waveguide embedded 250 GHz quasi-optical frequency-tripler array," *EuMC*, Oct. 2014.
- [B] **R. Dahlbäck**, T. Rubaek, M. Persson, and J. Stake, "A System for THz Imaging of Low-Contrast Targets Using the Born Approximation," *IEEE Transactions on Terahertz Science and Technology*, vol. 2, no. 3, pp. 361-370, April 2012.

The following publications are not included due to an overlap in contents or the contents are beyond the scope of this thesis:

- [C] J. Stake, H. Zhao, V. Drakinskiy, T. Bryllert, A Malko, J. Hanning, A.Y. Tang, P. Sobis, **R. Dahlbäck**, and J. Vukusic, "Integrated diode technology for THz applications," Presented at the *SPIE Optics+ Photonics, Terahertz Emitters, Receivers, and Applications IV*, Aug. 2013.
- [D] J. Stake, T. Bryllert, **R. Dahlbäck**, V. Drakinskiy, J. Hanning, A Malko, A.Y. Tang, J. Vukusic, H. Zhao and P. Sobis, "Integrated terahertz electronics for imaging and sensing," Presented at the *Microwave Radar and Wireless Communications (MIKON), 19th International Conference on*, May. 2012.
- [E] T. Rubæk, **R. Dahlbäck**, A. Fhager, M. Persson and J. Stake, "A single-channel THz imaging system for biomedical applications," Presented at the *General Assembly and Scientific Symposium, URSI* , Aug. 2011.
- [F] **R. Dahlbäck**, J. Vukusic and J. Stake, "Development of a waveguide integrated sub-millimetre wave spatially power combined HBV multiplier," Poster presented at the *6th ESA Workshop on Millimetre-Wave Technology and Applications and 4th Global Symposium on Millimeter Waves*, May. 2011.
- [G] T. Rubæk, **R. Dahlbäck**, A. Fhager, J. Stake and M. Persson, "A THz imaging system for biomedical applications," Presented at the *5th European Conference on Antennas and Propagation, EUCAP*, Apr. 2011.
- [H] **R. Dahlbäck**, T. Rubæk, T. Bryllert, M. Persson, and J. Stake, "A 340 GHz CW non-linear imaging system," Poster presented at the *Infrared Millimeter and Terahertz Waves (IRMMW-THz), 35th International Conference on*, Sep. 2010.
- [I] **R. Dahlbäck**, B. Banik, P. Sobis, A. Fhager, M. Persson, and J. Stake, "A Compact 340 GHz Heterodyne Imaging System," Presented at the *GigaHertz Symposium*, Mar. 2010.

Acknowledgement

First of all I would like to express my gratitude to my examiner and supervisor Prof. Jan Stake and my assistant supervisor Dr. Josip Vukusic who have given me support and the opportunity to work in this exciting field. My co-supervisors Dr. Tomas Bryllert and Dr. Peter Sobis have guided me through many technical difficulties for which I am grateful. I would also like to thank Johanna Hanning, Arvid Hammar and all colleagues at the Terahertz and Millimetre Wave Laboratory for giving me such a fun and inspiring work environment. Without Carl-Magnus Kihlman and his machining experience many of my crazy ideas had not been possible to realise. Catharina Forssen and the administrative staff at the Department of Microtechnology and Nanoscience deserves a special thank for making all my projects run smoothly.

I would also like to thank Dr. Tapani Närhi at ESA for helpful discussions on the topic of frequency multiplier 2D arrays.

I am grateful to Prof. Robert M. Weikle II who gave me the opportunity and guidance to deepen my knowledge in unit-cell modelling and quasi-optical measurements during my five months at the University of Virginia. A special thank goes to Alexander Arsenovic, Matt Bauwens, Michael Cyberey and all my colleagues at UVa for making my stay unforgettable.

Last but not least I would like to thank my fiancée Edna for all her love and support during this work.

This research was financially supported by the Swedish Research Council, VR, the European Space Agency, ESA and The Swedish Foundation for Strategic Research, SSF.

Robin Dahlbäck

*Göteborg
May 2014*

Table of Contents

Abstract	i
List of papers	iii
Acknowledgement	v
1 Introduction	1
2 Background	5
2.1 Varactor frequency multipliers	6
2.1.1 Non ideal varactors	7
2.1.2 Varactor multiplier matching	9
2.2 2D array of frequency multipliers	9
2.2.1 2D array of frequency multipliers enclosed in a waveguide cavity	10
3 Design of waveguide enclosed frequency multiplier grid arrays	13
3.1 Design of a 249 GHz waveguide embedded HBV grid array	13
3.1.1 Filters and matching elements for waveguide cavity operation . .	15
3.1.2 Waveguide cavity design	16
3.1.3 Filters and matching elements for free space operation	18
4 Fabrication and characterisation	21
4.1 Waveguide measurement setup	21
4.2 Free space measurement setup	23
5 THz imaging as an application for high power sources	27
6 Conclusions and future outlook	29
References	31

Chapter 1

Introduction

The THz region is one of the last unconquered parts of the electromagnetic spectrum. The difficulty of using this part of the spectrum comes from the fact that the frequency is very high in electronic terms but at the same time very low in the optical perspective; the terahertz gap is squeezed in between microwaves and visible light. The Terahertz region of the electromagnetic spectrum is generally defined as 300 GHz ($\lambda = 1 \text{ mm}$; photon energy = 1.2 meV) to 3 THz ($\lambda = 0.1 \text{ mm}$; photon energy = 12 meV).

Research on THz technology, was initiated by J. C. Bose who during the 1890's created the forerunner to modern diode detectors with his 60 GHz galena receiver [1]. The development of THz electronics has for long been led by the radioastronomy community, but is nowadays finding its way into a broader range of applications e.g. medical research [2], production monitoring [3], spectroscopy [4–11], non invasive inspection [12, 13] and security applications [14–16]. Common for all those fields is the lack of compact, efficient and affordable signal sources and detectors.

Power generation devices operating in the THz spectrum can be categorised into two main groups, electronics based devices and photonics based devices. The electronics based devices can further be subdivided into semiconductor devices and vacuum devices. The work presented here fall into the first category where distinct characteristics are that power is generated in a semiconductor, typically a diode or a transistor, and the circuit is designed using methods common for the microwave electronics community. Vacuum devices utilises the interaction of a relativistic electron beam with a slow wave structure to generate or amplify THz radiation [17]. Photonics based devices could be a semiconductor crystal where the THz generation comes from photo mixing, or quantum cascade lasers [18, 19].

One of the main advantages with electronics based sources is that they can operate in room temperature without cryocoolers or bulky high vacuum systems, a feature that

is highly desirable in many applications.

While signal sources for driving single channel receivers exist throughout the THz range applications such as 3D radars [14], communication links [20], NMR spectroscopy [21], research setups and imaging systems, such as the one featured in Paper B, call for an increasing amount of input power. Traditionally this problem has been addressed either by increasing the number of devices used on the multiplier chip or by waveguide based power-combination of several multipliers. However today's high power GaN amplifiers operating in the sub-THz region are providing more input power than traditional approaches effectively can handle. 2D array power combined frequency multipliers is a potential solution due to their high power handling capacity. Especially the first stage in a THz multiplier chain needs to handle high input powers, a fact that is illustrated in Figure 1.1.

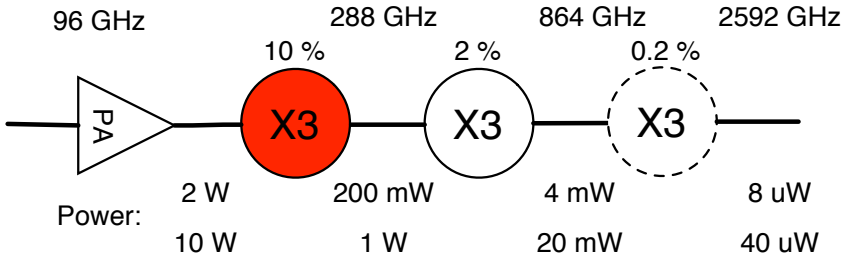


Figure 1.1: 2D array power combined frequency multipliers may be an alternative for the first stages in a high power THz source.

High power multipliers are needed when the frequency is too high to use amplifiers, today that breakpoint is approximately 300 GHz. Combined with the recent advancements in GaN amplifier technology around 100 GHz, [22–24], the settings are well suited to develop a high power frequency multiplier delivering record power levels around 300 GHz.

The highest output power and efficiency among frequency multipliers used today is found in diode based passive designs, a summary of current state of the art performance can be found in Figure 1.2. MMIC transistor technology has in recent years been making its way into the lower part of the THz region [25]. However for the highest frequencies and highest power levels diode based multipliers still holds a dominant position. Most commonly used are GaAs Schottky-diode multipliers and InP HBV-diode multipliers.

To achieve higher power levels in traditional planar design of frequency multipliers two main routes exist. The first one is to add more diodes in series or parallel on the chip, a method that works well up to around ten diodes [18, 26]. When the number

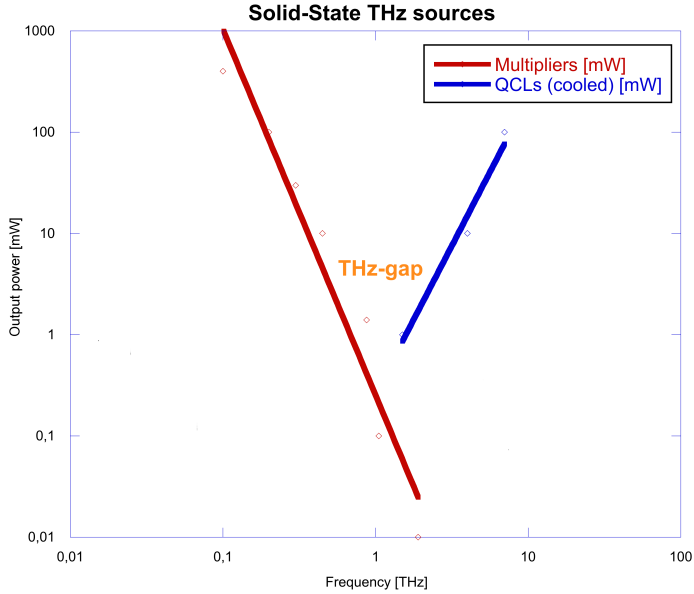


Figure 1.2: Output power levels for state-of-the-art sources, solid-state devices, in the THz frequency range [18, 19]. The term THz-gap is often used to describe the lack of powerful sources at THz frequencies.

of diodes increase so does the loss and complexity in the matching network. The other path is to use a waveguide split and combine network to power combine many multiplier circuits [18, 27–30]. This method also works well for a small number of chips but as the number of circuits increase the split and combine losses becomes dominant. Planar 2D arrays has an advantage, since the split and combine loss is independent of the number of devices, for networks with many (> 10) diodes [31]. A number of examples of free space operating 2D array frequency multipliers exist see e.g. [32–37]. Quasi-optical frequency multipliers with fewer active elements have also been presented [38–40]. The downside of free space arrays is that the in- and output coupling needs to be done quasi-optically using focusing elements which leads to a bulky system. Waveguide embedded 2D arrays are far less developed, [41, 42], but offers a compact unit compatible with existing waveguide based system. Waveguide embedded 2D array multipliers promises high output power, efficient power combining of a large number of devices and reliability through graceful degradation [31, 43].

Chapter 2

Background

Frequency multipliers at THz and sub-mm wave frequencies can be realised in a great number of ways. The field of varactor frequency multipliers has a long heritage and detailed textbooks covering the topics were available as early as the 1960s e.g. [44] by P. Penfield and R. P. Rafuse.

This thesis will focus on two terminal semiconductor device based multipliers, with special emphasis on multipliers using Heterostructure Barrier Varactor (HBV) diodes [45]. In general semiconductor diodes can operate as a frequency multiplier either by modulation of the nonlinear bias dependent depletion region capacitance, under reverse bias, or by modulation of the non linear forward conduction, during forward bias. Varistor and varactor mode operation each dominate at the respective boundaries of the diodes bias region but a combination of the two nonlinear effects may be used as well.

The main advantage of a varactor frequency multiplier is the high conversion efficiency, in theory 100 % for a lossless varactor [46]. Resistive multipliers have the advantage of a less reactive matching network leading to a greater operating bandwidth but suffer from an inherently lower conversion efficiency. The theoretical limit of conversion efficiency for a resistive multiplier is $1/n^2$, where n is the multiplication factor [47].

The nonlinear, voltage dependent, forward conductance or depletion region capacitance of Schottky diodes is often used at THz frequencies to realise frequency multipliers. In this work however heterostructure barrier varactor diodes, HBVs, one of the main competitors to Schottky diodes have been used.

2.1 Varactor frequency multipliers

The simplest varactor model introduced in [48] and drawn in Figure 2.1 contains only a voltage dependent capacitance in series with a constant parasitic resistance.

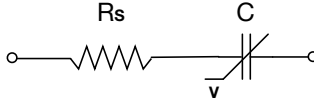


Figure 2.1: Uhler's varactor model containing the voltage dependent capacitance in series with a parasitic resistance.

The key to varactor multiplier operation is that the capacitance of the diode varies with the applied voltage. When driven, commonly referred to as pumped, by a signal source of frequency f_p harmonics of the input frequency, $f_{n \times p}$, will be generated.

When using a single Schottky-, PN- or similar diode a voltage dependent differential elastance $S=1/C$, where C is the capacitance, curve of the "Schottky shape" in Figure 2.2 is obtained. For varactor operation the diode is DC-biased somewhere in-between the reverse breakdown voltage and forward conduction threshold, typically around $V_{BD}/2$.

HBV diodes and other varactors with a symmetric elastance modulation function exhibit the behaviour illustrated by the "HBV line" in Figure 2.2 where the elastance is an even function around the zero bias point. If a varactor with an even elastance function and an odd conduction current function is operated around its point of symmetry only odd harmonics of the pump frequency will be generated.

When designing frequency multipliers a model of the diode behaviour is necessary. A good approximation for the charge dependent voltage over the particular HBV diode used in this work is the cubic varactor model, Equation (2.1), suggested by [49].

$$V(q) = S_{min}q + (S_{max} - S_{min})\left(\beta \frac{q^3}{q_{max}^2}\right) \quad (2.1)$$

Where V is the voltage over the varactor as a function of the applied charge, q . S_{max} and S_{min} the varactors maximum and minimum elastance, q_{max} the maximum charge and β a fitting parameter.

As the design work proceeds more and more elements are usually added to the model to improve the accuracy of the simulation. The shape of a varactors capacitance curve is directly coupled to the semiconductor design used and varactor optimisation is a topic in itself [50]. In [51] the effect of the shape of the elastance curve, coupled to different epitaxial structures, upon multiplier efficiency for symmetric varactors was investigated.

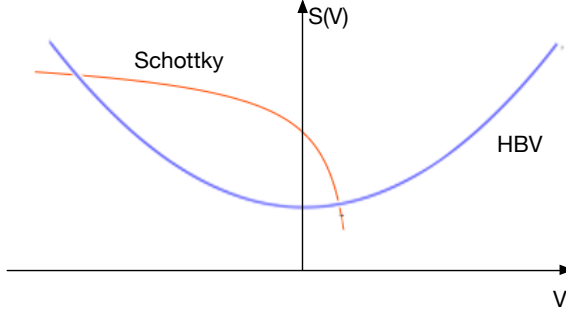


Figure 2.2: Typical differential elastance curves as a function of bias voltage for Schottky and HBV varactors.

2.1.1 Non ideal varactors

Even though the ideal varactor models in Figure 2.1 serves as a good starting point for a multiplier design parasitic effects needs to be included to accurately predict the performance of a THz frequency multiplier. An upper limit of the attainable performance of a varactor multiplier can be related to the dynamic cutoff frequency which relates the magnitude of the elastance modulation to the parasitic series resistance, R_S :

$$f_c = \frac{S_{max} - S_{min}}{2\pi R_s} \quad (2.2)$$

The dynamic cutoff frequency is a useful figure of merit when comparing varactor candidates for a multiplier design. It is also commonly used to evaluate tradeoffs when designing the epitaxial structure or mesa layout of a varactor diode.

A more elaborate model of an HBV diode is presented in Figure 2.3. It includes the voltage dependent capacitance, for which the cubic model in Equation (2.1) is a good approximation, the voltage and temperature dependent conduction current, and two parasitic elements. The parasitic series inductance originates mainly from the air-bridges, see Figure 2.4 for the geometry of a typical planar HBV diode. The parasitic series resistance has three main contributions:

- Bulk resistivity in the modulation layers, where the extension of the depletion region is voltage dependent, and the buried contact layer.
- Contact resistance.
- Ohmic losses in the connecting air-bridges which are frequency dependent due to the skin effect.

2. BACKGROUND

At high frequencies and high powers the finite electron velocity in the semiconductor material will influence the performance through current saturation effects [52]. High power levels will also increase the conduction current, acting as a parasitic varistor in parallel with the varactor. If the drive level exceeds the varactors reverse breakdown voltage the conduction current will increase rapidly leading to an effective decrease in conversion efficiency since resistive harmonic generation is far less effective than reactive. An other problem with high power levels is the self heating of the diode which also degrades performance [53].

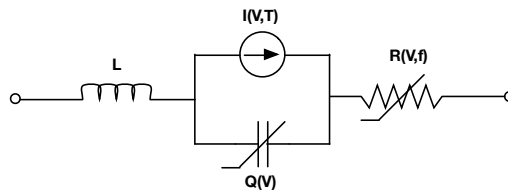


Figure 2.3: An HBV model including a voltage dependent conduction current, voltage and frequency dependent series resistance and a parasitic inductance.

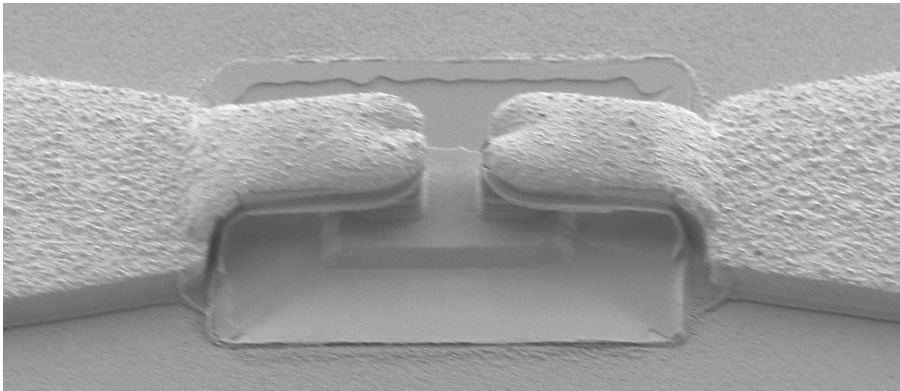


Figure 2.4: Scanning electron microscope picture showing a typical HBV diode consisting of two three-barrier mesa stacks contacted by air bridges at the top and a buried buffer layer in-between at the bottom.

2.1.2 Varactor multiplier matching

By optimising the source and load impedance at the input and desired harmonic frequency a large portion of the input power can be converted to the output frequency, ideally 100% for a lossless varactor without parasitic elements. The source and load impedances are generated by filter structures at the in and output, see Figure 2.5 for a two-port transmission line representation of a single HBV diode frequency multiplier. Since both in and output circuits interact the impedances in a final design is often based on a number of compromises, typically the impedance presented to the varactor at the input frequency has a greater effect on final performance. Besides the pump frequency and the desired output harmonic it may be necessary to terminate other harmonics with suitable impedances, referred to as *idler circuits* [54]. An example would be if a single non-symmetric varactor is to be used as a frequency tripler the second harmonic idler and possibly also the fourth harmonic idler would need to be terminated with proper idler circuits. Similarly for an HBV diode operating as a quintupler where the performance is greatly improved if the third harmonic is terminated in a reactive idler circuit [51].

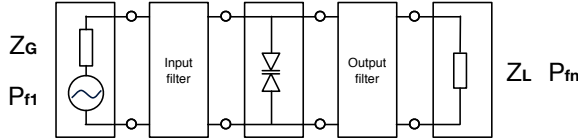


Figure 2.5: Two port models of a shunt mounted HBV diode together with input and output filters. The pump frequency is injected through the source at the left side and the power generated at the desired harmonic frequency is absorbed in the load at the output.

2.2 2D array of frequency multipliers

One of the main motivations for building 2D arrays of frequency multipliers is to increase the power handling capacity of the assembled frequency multiplier. The traditional circuit design methods struggle when the number of diodes in the multiplier approaches ten. In a 2D array of frequency multipliers an arbitrary grid size of $m \times n$ frequency multipliers can be chosen without affecting the power combining loss, however the advantage in terms of power handling compared to traditional power combined designs increase as the total number of devices increase [31].

The most common approach when designing large arrays of identical elements is to model the device using the unit cell approach. When doing so, periodic electric and magnetic boundary conditions are enforced on the borders of the symmetric cells,

assuming an infinite array of identical elements operating in phase. In this way the computational burden can be reduced to solving a single cell. In reality no arrays are infinite in size but the method has proven useful even for relatively small arrays.

Simpler unit cell structures can with good accuracy be approximated using the induced electromagnetic force (EMF) method, described in [55, 56], which is a development of the work by Eisenhart and Kahn [57]. This approach has the advantage that a lumped element model with analytical expressions relating to the unit cell dimensions can be created. For the initial design work this can be a very useful tool to find a good starting point for more precise 3D EM simulations, that later can replace the EMF model. For more complex geometries where the basic assumptions in the EMF method becomes too complex a full wave commercial 3D EM field solver may be used directly to create the unit cell model.

A quasi-optical multiplier array usually consist of a number of components that can be approximated using the unit cell approach e.g. input filter, the active array and output filter. It was shown in [58] that several arrays containing unit cell models could be cascaded using transmission line theory. By applying that approach well known transmission line techniques can be applied when designing the input and output matching networks. As an example a plate with a predetermined thickness that is inserted in the path of the propagating wave will act as a transmission line with a wave impedance determined by the permittivity, assuming lossless and nonmagnetic materials, of the material and electrical length determined by the thickness.

Care must be taken when modelling cascaded arrays since the model does not include evanescent coupling between the arrays. In practice this means that e.g. two metallic filter surfaces can not be modelled separately and then be put into the transmission line model right next to each other since the evanescent field coupling that occurs between the filters is not included in the transmission line model. As a rule of thumb evanescent coupling can be expected to occur if the distance between the elements is a small fraction of the guided wavelength. Metallic patterns such as antennas and filters must also be modelled with the correct dielectric backing, which later can be de-embedded, in order to correctly account for the added capacitance in e.g. gaps.

This modelling approach enables the use of different sized unit cells in cascade and individual elements can be represented either by approximate lumped component models or more exact numerical simulation files. The thickness of substrates and air-gaps can also easily be used as tuning parameters in the model, an example of a typical transmission line model of an array multiplier is shown in Figure 2.6.

The model in Figure 2.6 is usually solved using a Harmonic Balance simulator to evaluate the expected frequency multiplier performance.

2.2.1 2D array of frequency multipliers enclosed in a waveguide cavity

Many quasi-optical multiplier arrays published, e.g. [59–61], are tested by illuminating the arrays in the antenna far-field of a high power source. Such a setup provides a nearly

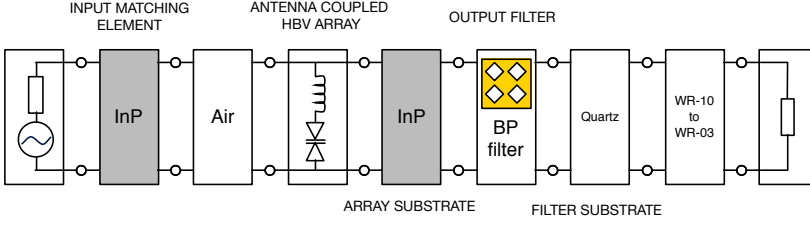


Figure 2.6: An example of a complete multiplier setup as a transmission line model for harmonic balance simulations.

plane wave at the array and thus makes the unit cell modelling fully valid, except for edge effects in the array itself, but also has the downside that most of the available pump power is lost due to spill-over. The overall system efficiency is therefore much lower than the reported array conversion efficiencies and the setups are unsuitable for system integration. Many of the systems presented also only samples part of the output beam to estimate the total output power, a method valid in itself but if the generated power was to be used in an actual system additional focusing elements may be needed.

One of the main advantages of packaging 2D arrays in waveguides is that it enables the integration into systems by means of standardised waveguide interfaces, operating with the TE_{10} mode. This also makes characterisation of the components easier since traceable calorimetric power meters exist in the THz band. However when packaging an array in a waveguide the uniform plane wave excitation assumed in unit cell modelling does not hold true. In a fundamental mode TE_{10} waveguide the e-field varies as $\sin x$, and the power density as $\sin^2 x$, with a constant phase along the broad waveguide dimension.

The work in this thesis and previous work within the field, [41, 42], are using a fundamental mode waveguide at the input frequency which then becomes over-moded at the desired harmonic. The uneven power distribution means that the elements of a symmetric uniform array will receive different input powers depending on their position in the array. It was suggested in [42] that the implications of this could be handled by calculating the input power to each individual varactor diode, estimate a conversion efficiency and finally sum the total output field. Since the conversion efficiency varies along one of the waveguide dimensions the output mode will not be a pure TE_{10} but instead a composition of TE modes.

One of the main practical differences when using the unit cell approach to model 2D arrays in waveguides is that the wave impedance seen on the two plane wave ports is frequency dependent while in a free space environment only the electrical phase length is frequency dependent. The wave impedance of the TE_{10} mode in a rectangular

waveguide is known to be:

$$Z_{TE_{10}} = \frac{Z_0}{\sqrt{1 - \left(\frac{f_c}{f}\right)^2}} \quad (2.3)$$

Where f_c is the cutoff frequency for the mode, f is the frequency and

$$Z_0 = \sqrt{\frac{\mu_0}{\varepsilon_0}} \approx 377\Omega \quad (2.4)$$

in vacuum. From Equation (2.3) it is clear that as the frequency increase the wave impedance in the waveguide will approach that of a free space propagating wave. It also means that for a 2D array multiplier in a waveguide environment the fundamental frequency and harmonic frequency will experience different wave impedances and the difference between the fundamental frequency and the harmonic frequency will be less if the wave propagates through e.g. a dielectric matching plate with high permittivity.

The modelling approach used in this thesis is to apply the unit cell concept to the array and filter element and use the wave impedance presented by the waveguide in the harmonic balance simulations. The uneven power density distribution in the waveguide is only accounted for in the total efficiency calculations for the complete multiplier array, not during the unit cell design which means that in practice the unit cell assumption of perfect periodic boundaries becomes less accurate.

Chapter 3

Design of waveguide enclosed frequency multiplier grid arrays

Most frequency multiplier 2D arrays presented so far have been designed for free space operation, sometimes also referred to as open structures, where the in and output signals are coupled to the circuit quasi-optically. Either by illuminating the array in the far field of an antenna where the incident field can be well approximated by a plane wave or by using focusing optics and thereby provide a Gaussian shaped power density across the target array. The modelling of free-space arrays is more developed than for the waveguide embedded arrays and experimental data exists to verify, cf. [59–61]. However many experiments with free space arrays have been performed by illuminating the array in the far field of a high power source e.g a free-electron laser. By doing so the plane wave illumination condition assumed in the unit cell modelling is fulfilled but only a small fraction of the pump source output power couples to the the array, so even though the array conversion efficiency is quite good the overall system efficiency is very low. It is generally hard to provide an even illumination without suffering from large spillover losses. Also, the downside of free space arrays is that the total setup becomes bulky and less flexible compared to a waveguide packaged component. In addition, the electronics community, used to standardised waveguide interfaces between components, rendering open quasi optical solutions impractical for applied system design.

3.1 Design of a 249 GHz waveguide embedded HBV grid array

The design of any type of frequency multiplier is an iterative process. Many interactions exist between different design parameters and a number of tradeoffs need to be balanced against each other. Typical input parameters for a design may include input and output

3. DESIGN OF WAVEGUIDE ENCLOSED FREQUENCY MULTIPLIER GRID ARRAYS

frequency, bandwidth, output power and conversion efficiency. In this design, presented in Paper A, HBV diodes based on the epi-stack design from [62] was used. Besides the varactor material chosen a design input was that an available 83 GHz 1 W GaN power amplifier was to be used to pump a tripler multiplier 2D array. It was also desirable to build an array that could be tested both in free space operation as well as in a waveguide cavity, the motivation to this was to gain experience in both types of designs.

The unit cell size chosen for this design is $211 \mu\text{m}$ which gives a 12 by 6 element 2D array if mounted in a standard WR-10 waveguide. A WR-10 waveguide was chosen on the input side since this meant that no additional input waveguide taper had to be manufactured which made testing easier.

The compromises accounted for in the waveguide case was to use a unit cell large enough to receive sufficient power for efficient varactor frequency multiplication but at the same time be small enough not to excite higher order modes. Given the unit cell dimensions and the available input power an HBV varactor optimised to operate with 20 mW input power at 83 GHz was designed. With the epitaxial material used this resulted in the $30 \mu\text{m}^2$, two mesa, six barrier HBV varactor shown in Figure 2.4.

A dipole like antenna structure was chosen for the antenna array after many iterations between a Finite Element Frequency Domain solver, used to simulate the unit cell, and a Harmonic Balance circuit solver, used to simulate the entire multiplier circuit. A lumped element model of the unit cell was produced using the induced EMF method, both models can be seen in Figure 3.1.

The designed unit cell is expected to yield a conversion efficiency of 10 % for an input of 20 mW if supplied with correct embedding impedances. The number given assumes some losses in the matching network that seemed reasonable during the design, the intrinsic conversion efficiency is somewhat higher.

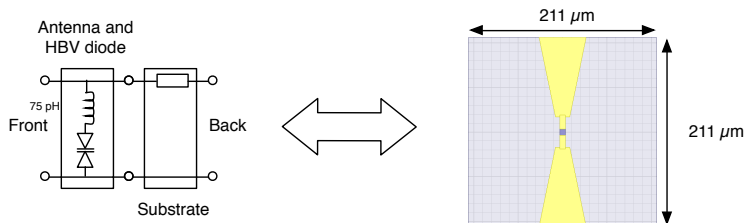


Figure 3.1: An analytical two-port transmission line model, from the induced EMF method, together with the equivalent unit cell used for FEM modelling. The yellow part of the unit-cell represent the antenna metal structure, where the HBV varactor is positioned in the centre.

3.1.1 Filters and matching elements for waveguide cavity operation

To realise the embedding network needed for optimum frequency multiplier operation a combination of dielectric matching slabs and a bandpass filter was used. Since both the input frequency and the third harmonic propagate in the same environment all matching elements except the last quartz slab at the output affect the varactor embedding impedance on both harmonics. It can therefore be hard to separate the effect of the different components in the matching network, presented in Figure 3.2, but some general properties will be outlined.

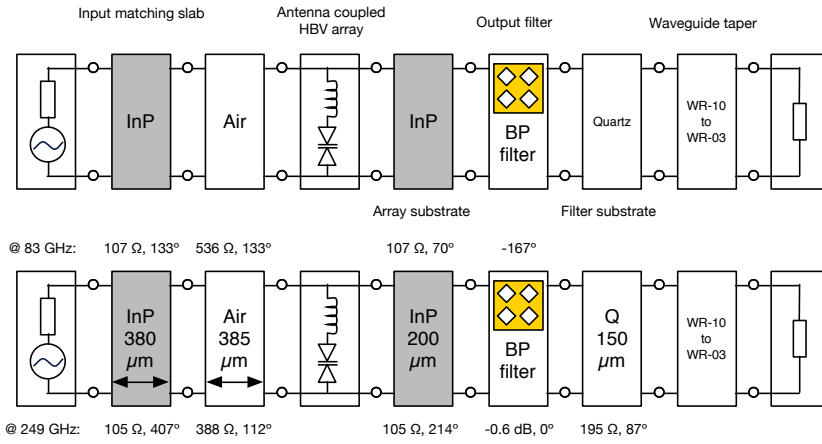


Figure 3.2: A complete unit cell transmission line model of the frequency tripler 2D array. The model at the top describes the functional blocks and the bottom version of the same circuit provides details about the electrical properties.

Starting from the input side of the multiplier a piece of InP substrate is used to match the input signal and thereby maximise the power transfer to the diodes. A summary of the wave impedances in a WR-10, TE_{10} waveguide environment for the materials used is given in Table 3.1 for reference.

To create the filter needed for efficient multiplier operation a dielectric backed metal surface with a periodic metal pattern was used, commonly referred to as frequency selective surface. The design of frequency selective surfaces, or filters, is well covered in the literature [63]. Important aspects when designing a filter is to consider the wave impedances on both sides which is dependent on if a dielectric support substrate is used or not. The filters resonance frequency will also be affected by the surrounding wave impedances, i.e. the resonance frequency for a planar periodic filter mounted in a

3. DESIGN OF WAVEGUIDE ENCLOSED FREQUENCY MULTIPLIER GRID ARRAYS

Material	Wave impedance [Ω]		
	83 GHz	249 GHz	Free space
Air	536	388	377
InP	109	107	105
Quartz	208	195	193

Table 3.1: TE_{10} wave impedance in a WR-10 waveguide filled with a dielectric at the two critical frequencies in the design and complementary data for a free space propagating wave.

TE_{10} mode waveguide will differ from the same filter resonance frequency in free space operation. The design used here uses a Rhombic aperture bandpass filter fabricated on a quartz substrate at the output to pass the third harmonic and reflect the first harmonic. The output filter together with the array substrate serves many purposes, see Figure 3.3:

- Acts as a back-short at the input frequency; The substrate roundtrip phase plus the reflection phase of the filter at f_1 should add to 0 (or $n \times 2\pi$).
- Matches the output frequency, f_3 , with minimum loss.
- Transfers the propagating f_3 to the output waveguide impedance; The quartz substrate acts as a $\lambda/4$ transformer between the InP array substrate and the air filled WR-10 waveguide.
- Transfers heat from the array to the metal waveguide block.

Since the filter also serves as a heat-sink to the array so the thermal properties of the dielectric chosen for the filter needs to be considered, especially for the high power application 2D arrays we aim for. Here quartz was chosen since thermal simulations predict that the InP substrate of the device array in itself provided sufficient heat dissipation for the given application and the impedance of the quartz substrate is close to the geometric mean of the air filled waveguide and the InP varactor substrate at the third harmonic making it suitable as a $\lambda/4$ output impedance transformer.

3.1.2 Waveguide cavity design

The most common way of realising multipliers and other THz circuits is by what is commonly referred to as E-plane split blocks. A waveguide block machined in this fashion typically consists of two milled halves where the waveguide has been split along the E-field symmetry plane, for the TE_{10} mode standard rectangular waveguide with a 2:1 ratio between the walls this means that the two halves will have a quadratic cut. Since no surface currents flow across this plane on the waveguide wall the method is rather insensitive against poor electrical connection between the waveguide halves. Conventional THz circuits are typically mounted in one of the waveguide block halves and couple to the propagating wave in the waveguide by E or H field probes. When

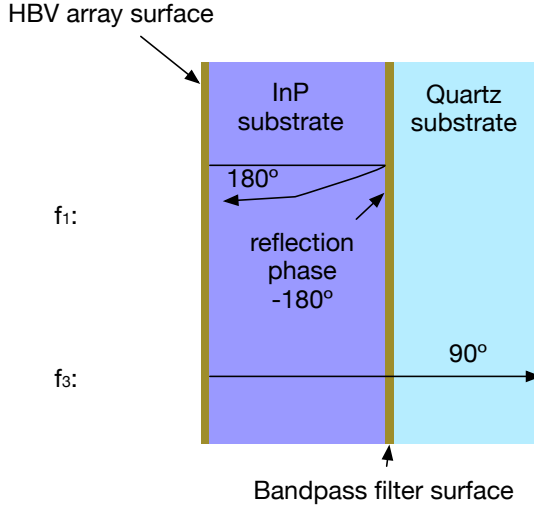


Figure 3.3: Cross section view of the array stack. From left to right: the 2D HBV array on a InP substrate followed by the bandpass filter structure on a quartz substrate. The properties are described by two rows explaining the function, one for the input frequency, f_1 and one for the third harmonic frequency f_3 .

mounting such circuits all work can be done in one of the halves and then the other half of the waveguide can be attached.

The fabrication of waveguide packaged components becomes increasingly difficult at frequency approaching the terahertz region. One of the main reasons for this is that the waveguide dimensions shrink to the order of hundreds of micrometers making it hard to machine with sufficient precision and surface finish even when using modern computer controlled mills. Assembling such circuits with high yield requires precision in the micrometer range.

For quasi optical components designed to couple directly to the propagating wave the E-plane split block manufacturing technique described earlier becomes problematic. If all components are mounted in one half of an E-plane split block extreme care must be taken when mounting the other waveguide half or the arrays will be shattered. An other problem is the poor thermal contact since there is no natural way of thermally attaching the waveguide to the multiplier chip. One approach could be to apply the waveguide split in an other plane e.g. as in [41], but at frequencies in the THz range such waveguide split can cause large ohmic losses and degrades efficiency.

In this work a shim system has been used instead where the different parts are mounted in interchangeable shims. Since the shims are relatively thin, tooling exist to machine the shims from the direction of the propagating wave, making machining

3. DESIGN OF WAVEGUIDE ENCLOSED FREQUENCY MULTIPLIER GRID ARRAYS

easier. Figure 3.4, also present in Paper A, shows an assembled multiplier unit, 3.4b, consisting of one shim holding the input matching slab, one shim housing the array, output filter and output matching finally followed by a WR-10 to WR-03 waveguide taper. In Figure 3.4a the shim that holds the the array, output filter and output matching slab is shown before assembly. After the parts are inserted in the shim a thermal glue is applied in the round corner pockets and along the short side of the array, securing the assembled package in the shim and enhancing thermal conduction.



(a) Mounting shim, HBV 2D array, bandpass filter and Quartz matching slab



(b) Complete assembled multiplier unit

Figure 3.4: Two pictures showing the shim concept, from Paper A.

3.1.3 Filters and matching elements for free space operation

For free space operation a simpler matching circuit made for plane wave operation is designed. It is based on two available commercial bandpass filters fabricated as a copper foil. One filter has its centre frequency at the 83 GHz input tone and the other at the 249 GHz output harmonic. Since no simulation data was available for the filters the matching strategy is to have a setup where the distance between the filters and the array can be varied, thereby finding the positions where the output filter acts as a back-short for the input harmonic and the input filter reflects the part of the third harmonic that propagates in the wrong direction.

The full varactor substrate thickness of $635\mu\text{m}$ is used in the matching circuit that can be seen in Figure 3.5

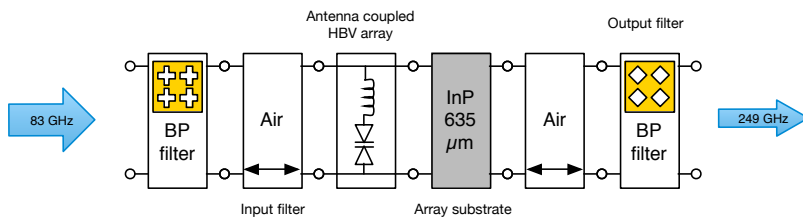


Figure 3.5: A complete unit cell transmission line model of the free space operating frequency tripler 2D array. Two position adjustable bandpass filters are used to tune the circuit.

Chapter 4

Fabrication and characterisation

The HBV 2D arrays were fabricated using the same method as described in [64]. Two chips have been made to date, each containing twenty 6 x 12 unit-cell 2D arrays suited for WR-10 waveguide mounting and two 33 x 33 arrays for free space tests. The 6 x 12 2D arrays were then sawed into 2.54 mm x 1.27 mm dies and lapped to 200 μm thickness resulting in arrays as the one in Figure 4.1. A scanning electron microscope picture of a part of the array is also shown in Figure 4.2. The results from the first chip fabricated is presented in Paper A, while the results from the second chip are presented in this chapter.

4.1 Waveguide measurement setup

To characterise the arrays a measurement setup built around a 83 GHz GaN power amplifier was built, a block diagram is shown in Figure 4.3. The power amplifier is fed through a chain consisting of a microwave synthesiser, a x6 frequency multiplier, two amplifiers and an isolator. On the output of the amplifier a circulator is attached to isolate the power amplifier from the sometimes highly reflective multiplier device under test (DUT). The return port of the circulator is simultaneously used to measure the reflected power, while the forward power is measured with a calibrated diode detector through the directional coupler. The output power from the DUT is measured by a calorimetric power sensor through a WR-03 to WR-10 waveguide taper. The first taper is used to create a single mode TE_{10} output from the frequency multiplier while the second taper matches the output of the multiplier to the WR-10 input of the power detector. The short section of WR-03 waveguide between the tapers also serves as a 170 GHz high-pass filter, effectively blocking any pump frequency signal from reaching the output power detector.

4. FABRICATION AND CHARACTERISATION

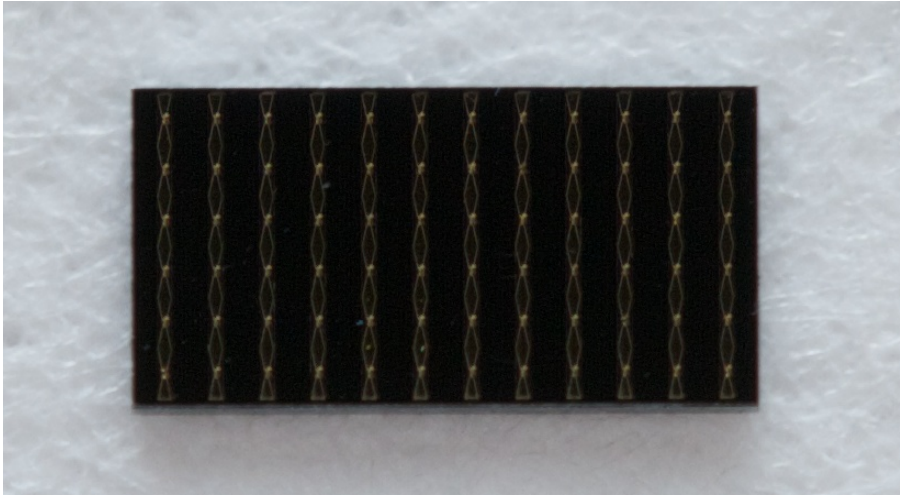


Figure 4.1: Photograph of a manufactured 6 x 12 array.

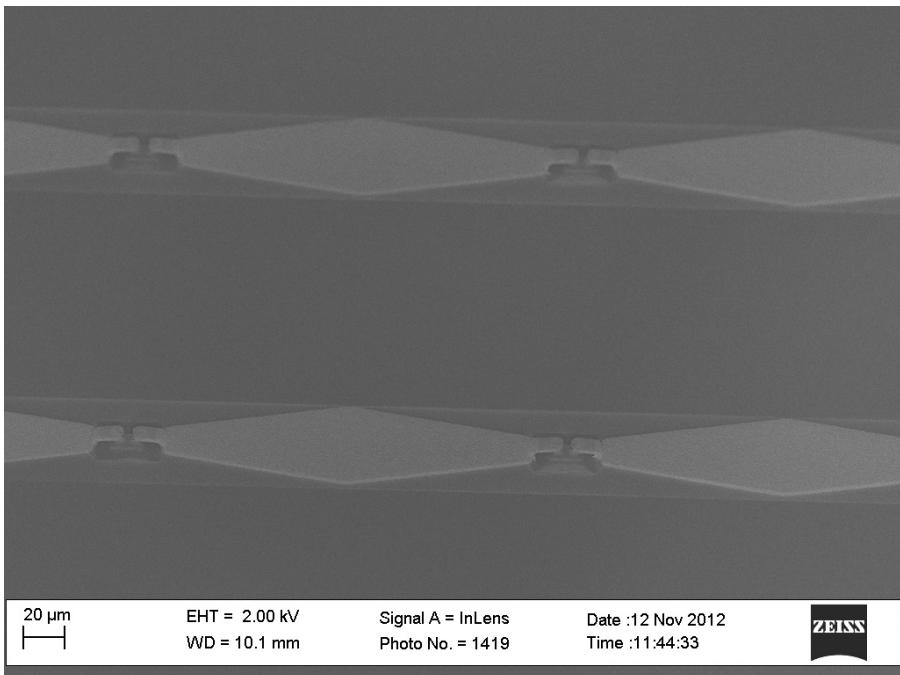


Figure 4.2: Scanning electron microscope picture of a part of the array. Note the four air-bridge contacted HBV varactor diodes.

Since the power amplifier is driven into saturation harmonics could potentially be generated and incorrectly interpreted as output signal from the multiplier. To test this the multiplier array was replaced with a dummy InP chip while the amplifier was operated under the same conditions as during the actual tests. The harmonic content was not measurable or $\ll 1\%$ of the measured output power from the multiplier. Another potential source of error are output signals from the multiplier at higher frequencies than the desired harmonic since the detector is sensitive well up at visible light frequencies. For the multipliers measured here the third harmonic is the desired output signal but some power may also be generated at higher odd harmonics. This has not yet been investigated though.

Infrared radiation, originating from chip heating during measurements has been excluded as an error source by comparative measurements with IR-absorbing material in the waveguide.

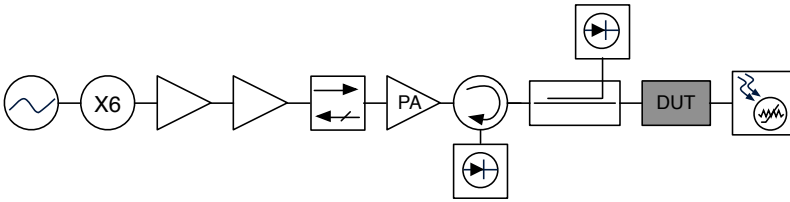


Figure 4.3: A block diagram of the measurement setup used to characterise the arrays.

The measurement result from one of the tested 2D arrays is shown in Figure 4.4, the data in the graph is from one of the 6×12 arrays. Within the batch of 20 arrays approximately five show similar performance as the one presented here while the rest produce lower output power and efficiencies. The diode yield of the measured chip has not been evaluated but it is expected to be better than the 70 % measured on the chip in Paper A. As can be seen in the graph the conversion efficiency, and output power is strongly dependent on the input power, as expected. It should also be noted that at some frequencies the multiplier is driven beyond its peak output power and that the output power is actually decreasing as the input increase.

4.2 Free space measurement setup

A measurement setup built to test the larger 33×33 array under free space conditions is shown in Figure 4.5. The output from the power amplifier is transmitted through a corrugated horn and then focused by two off-axis parabolic mirrors onto the HBV 2D

4. FABRICATION AND CHARACTERISATION

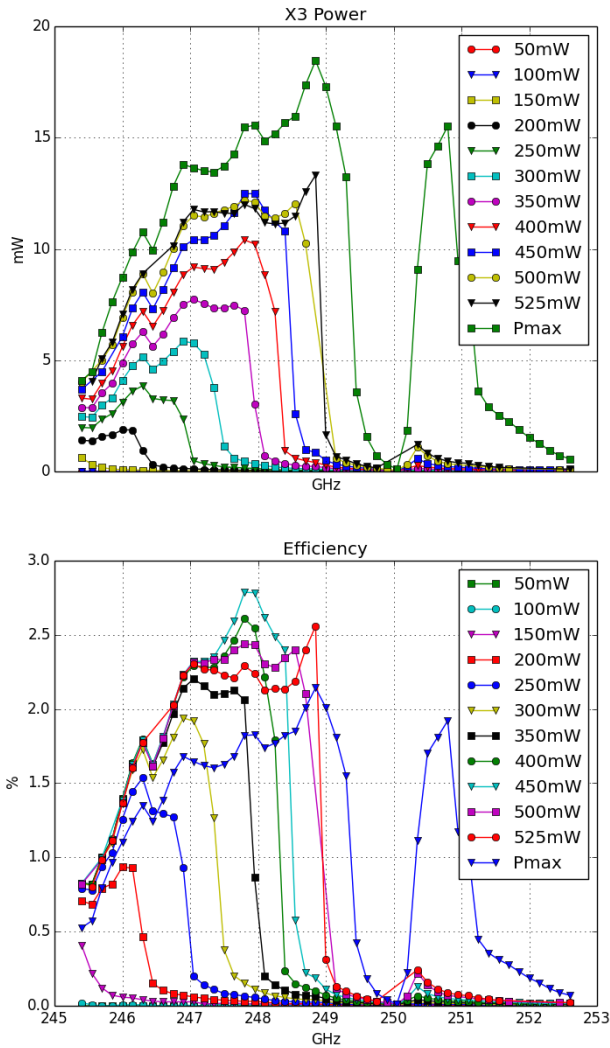


Figure 4.4: Plot showing the measured output power and conversion efficiency as a function of frequency. The Pmax label represent a measurement without the coupler measuring the forward power, to minimise input loss. The input power from that measurement has been estimated to have a peak of 860 mW at 83 GHz, corresponding to 249 GHz output frequency.

array. Surrounding the array are the two bandpass filters described in Section 3.1.3 mounted on linear adjustment stages enabling the distance between the filters and the array to be varied. The output power is sampled by a diode detector mounted on a three axis micrometer stage. By moving the stage the output beam was sampled in the E- and H-plane at various distances from the array. The output from the multiplier 2D array has a Gaussian power distribution, just as it is expected to be. By fitting a Gaussian beam to the measured data and then integrating the power in the fitted beam the total output power can be estimated to be 0.6 mW. This yields a very low conversion efficiency, approximately 0.1 %, that is explained by the fact that the input beam power density is Gaussian shaped and covers the 2D array with approximately 90 % spillover efficiency. Thus the power delivered to the individual varactors is low, explaining the low conversion efficiency.

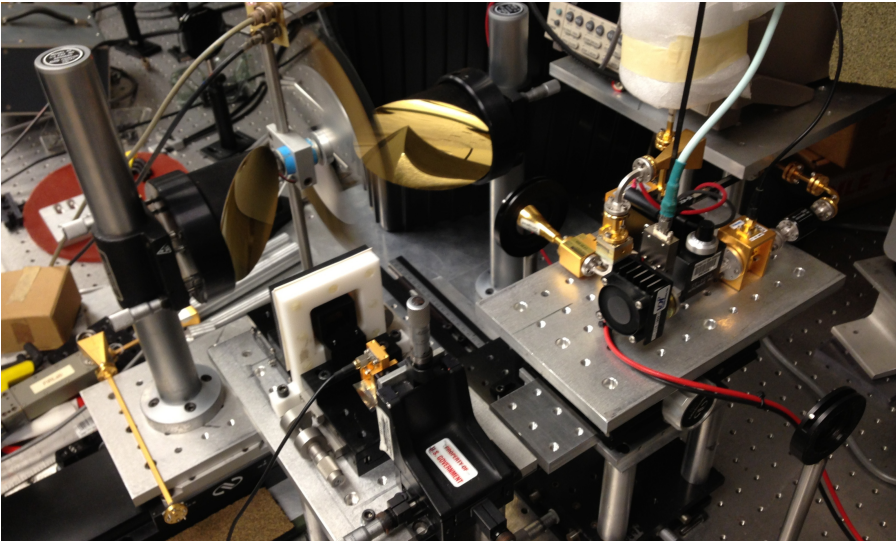


Figure 4.5: Photograph of the free space test setup, the 2D array under test is mounted in the white plastic holder in the left part of the image. The input power radiated from the horn antenna in the upper right part of the picture is focused to the array by two parabolic mirrors. Surrounding the array are the two adjustable filter holders. The diode detector used to sample the output power can be seen on the three axis adjustable stage.

Chapter 5

THz imaging as an application for high power sources

THz imaging has been applied in a large number of applications including biology and medicine [65–72], non invasive imaging [12, 13] and security screening [15, 16, 73]. In Paper B a THz imaging system built for biological sample investigation is presented. Samples of $200\ \mu\text{m}$ thickness can be scanned for contrasts in the dielectric properties. An image reconstruction algorithm based in the Born approximation is used to reconstruct the complex permittivity of the sample in the imaging region. The reconstruction algorithm used creates imaging voxels, three dimensional pixels, of $0.1 \times 0.1\ \text{mm}^2$ (approximately 1/10 of the free space wavelength) in the planar direction, and the whole thickness of the sample is assumed to have the same properties within the voxel.

To illustrate the performance of the imaging system an imaged leaf, from Paper B, together with measured raw amplitude data and reconstructed complex permittivity is shown in Figure 5.1. Biological samples often have a high concentration of water which means that they are very lossy at THz frequencies. This is the main reason for the $200\ \mu\text{m}$ sample thickness limit of the imaging system. The leaf used in this example was a bit dry, thus making it possible to image a slightly thicker sample with good results. With more input power, which is the goal of the work in this thesis, thicker samples with higher moisture content could be imaged. An other route towards more dynamic range is to increase the sensitivity in the receiver chain.

By having more power available at THz frequencies, the applicability of THz imaging would be widened, allowing for more diverse geometries and materials to be scanned with increased dynamic range.

The goal is to use the system to scan histopathological cancer samples and determine the tumour boundary. THz radiation is particularly suitable for this due to the higher

absorption of the water retentive cancerous tissue. Although acquiring test samples with appropriate thickness has so far been problematic.

These power requirements at THz frequencies could be met by the inherent power combining nature of 2D arrays of frequency multipliers. Arrays, such as the ones features in this report, could be utilised as a pump source at sub-mm (over 300 GHz) frequencies or as cascaded arrays to produce high power at THz frequencies. Thus making similar imaging setups as the one presented, with higher dynamic range, possible at even higher frequencies.

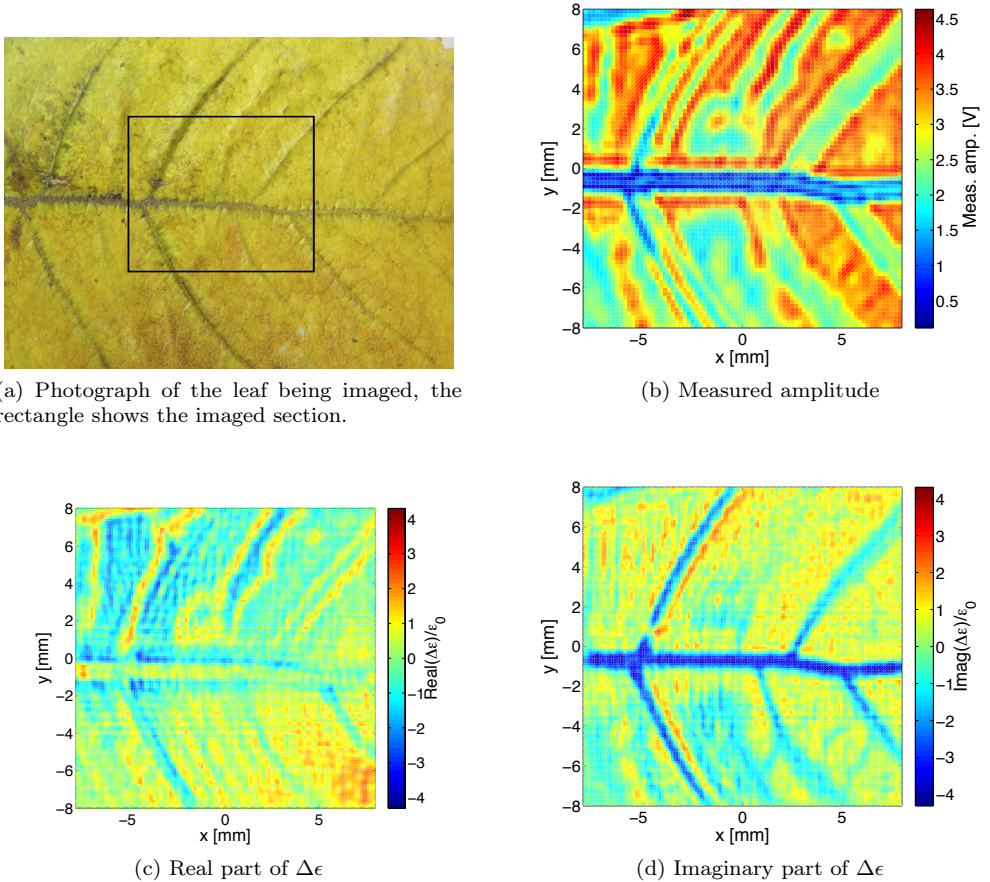


Figure 5.1: The leaf being imaged is shown in (a). The measured amplitude (unprocessed data) is shown in (b) and the real and imaginary parts of the contrast in relative permittivity are shown in (c) and (d). From Paper B.

Chapter 6

Conclusions and future outlook

There are many things that could be improved in the modelling of 2D multiplier arrays enclosed in waveguide cavities. It is a topic where many different assumptions have to be combined into a complex model. Using the unit-cell approach with the proper frequency dependent wave impedance, as used in this work, seems to give a reasonable agreement with measurements. One of the most difficult parts is to model the power transfer to the individual diodes in the 2D array. Since the impedance of a varactor diode does depend on the applied voltage, the neighbouring elements in the array will present different impedances to the antenna circuit. Furthermore, at the edges of the array, edge effects not accounted for in the unit-cell modelling will be present. The diode properties are also strongly temperature dependent making a complete system model truly multi disciplinary. If the individual diode excitation could be calculated a much better model for the third tone output in the over-moded waveguide could be calculated. With knowledge of the mode composition, since a pure TE_{10} is not expected, the output matching could be improved to pass more of the generated power.

Nevertheless a simple division of the power among the unit-cells based on the power density in the waveguide and their positions followed by individual conversion efficiency calculations and a simple summation predict that the peak conversion efficiency should be approx. 5% for the tripler in Section 4.1. A number that is in quite good agreement with the measured result especially since no compensation for losses in the output waveguide tapers have been added to the presented output power.

In the planned iterations of 2D array frequency multipliers the following topics will be addressed:

- Careful modelling of power lost to substrate modes and mode trapping [74].
- A full wave 3D EM simulation of the complete multiplier structure, including all nonlinear elements.
- More advanced array and filter structures.
- A design utilising polarisation separation instead of bandpass filters to separate the fundamental and desired harmonic frequencies.

The overall efficiency of the multiplier module would be greatly improved if the power could be more evenly divided among the varactor diodes. One way towards that is to use a non uniform array, where either the unit cell dimensions or the diode size change depending on the position in the array to account for the uneven power density of the input TE_{10} mode. The mode in the input waveguide could also be altered by loading the waveguide walls with either a dielectric or some sort of periodic structure, giving a more uniform power distribution for the central elements in the array. An other solution is to use a larger waveguide with a composition mode that exhibits a more uniform power density, as exemplified with a grid amplifier in [75]. That approach will however require much more available input power since the array will need to be much larger. There are many ways forward in the field of 2D frequency multiplier arrays, one of the most important being straight forward design methods. If a unified, accurate, design method could be outlined the technology has a great potential to provide the high power THz sources of the future.

References

- [1] D. L. Sengupta, T. K. Sarkar, and D. Sen, “Centennial of the semiconductor diode detector,” *Proceedings of the IEEE*, vol. 86, pp. 235–243, Jan. 1998.
- [2] E. Pickwell and V. P. Wallace, “Biomedical applications of terahertz technology,” *Journal of Physics D: Applied Physics*, vol. 39, pp. R301–R310, Aug. 2006.
- [3] P. F. Taday, “Applications of terahertz spectroscopy to pharmaceutical sciences,” *Philosophical Transactions of the Royal Society A: Mathematical, Physical and Engineering Sciences*, vol. 362, pp. 351–364, Feb. 2004.
- [4] F. C. De Lucia, “The submillimeter: A spectroscopist’s view,” *Journal of Molecular Spectroscopy*, 2010.
- [5] H. J. Hansen, “Standoff Detection Using Millimeter and Submillimeter Wave Spectroscopy,” in *Proceedings of the IEEE*, pp. 1691–1704, 2007.
- [6] N. Gopalsami and A. C. Raptis, “Remote detection of chemicals by millimeter-wave spectroscopy,” *SPIE’s International Symposium on Optical Science, Engineering, and Instrumentation*, vol. 3465, pp. 254–265, Nov. 1998.
- [7] N. Shimizu, H. J. Song, Y. Kado, T. Furuta, and A. Wakatsuki, *Gas detection using terahertz waves*. NTT Technical Review, 2009.
- [8] M. Tonouchi, “Cutting-edge terahertz technology,” *Nature Photonics*, vol. 1, pp. 97–105, Feb. 2007.
- [9] N. Gopalsami, S. Bakhtiari, T. W. Elmer II, and A. C. Raptis, “Application of Millimeter-Wave Radiometry for Remote Chemical Detection,” *IEEE Trans. Microwave Theory Tech.*, vol. 56, no. 3, pp. 700–709, 2008.
- [10] “Identification of chemicals in the vapor phase by directly measuring absorption spectra through frequency-tuning a monochromatic THz source,” in *Optics East* (J. O. Jensen and J.-M. Theriault, eds.), pp. 11–15, SPIE, Dec. 2004.

- [11] P. Buaphad, P. Thamboon, C. Tengsivattana, J. Saisut, K. Kusoljariyakul, M. W. Rhodes, and C. Thongbai, "Progress on Reflective Terahertz Imaging for Identification of Water in Flow Channels of PEM Fuel Cells," *Applied Mechanics and Materials*, vol. 110-116, pp. 2301–2307, Oct. 2011.
- [12] W. L. Chan, J. Deibel, and D. M. Mittleman, "Imaging with terahertz radiation," *Reports on Progress in Physics*, vol. 70, pp. 1325–1379, July 2007.
- [13] S. Kharkovsky, J. T. Case, M. A. Abou-Khousa, R. Zoughi, and F. L. Hepburn, "Millimeter-Wave Detection of Localized Anomalies in the Space Shuttle External Fuel Tank Insulating Foam," *IEEE Transactions on Instrumentation and Measurement*, vol. 55, pp. 1250–1257, Aug. 2006.
- [14] T. Bryllert, K. B. Cooper, R. J. Dengler, N. Llombart, G. Chattopadhyay, E. Schlecht, J. Gill, C. Lee, A. Skalare, I. Mehdi, and P. H. Siegel, "A 600 GHz imaging radar for concealed objects detection," in *2009 IEEE Radar Conference*, pp. 1–3, IEEE.
- [15] K. Cooper, R. Dengler, N. Llombart, T. Bryllert, G. Chattopadhyay, E. Schlecht, J. Gill, C. Lee, A. Skalare, and I. Mehdi, "Penetrating 3-D Imaging at 4-and 25-m Range Using a Submillimeter-Wave Radar," *IEEE Transactions on Microwave Theory and Techniques*, vol. 56, no. 12, Part 1, pp. 2771–2778, 2008.
- [16] C. Am Weg, W. von Spiegel, R. Henneberger, R. Zimmermann, T. Loeffler, and H. G. Roskos, "Fast Active THz Cameras with Ranging Capabilities," *Journal of Infrared, Millimeter and Terahertz Waves*, vol. 30, pp. 1281–1296, Aug. 2009.
- [17] J. H. Booske, R. J. Dobbs, C. D. Joye, C. L. Kory, G. R. Neil, G.-S. Park, J. Park, and R. J. Temkin, "Vacuum Electronic High Power Terahertz Sources," *IEEE Transactions on Terahertz Science and Technology*, vol. 1, no. 1, pp. 54–75.
- [18] G. Chattopadhyay, "Technology, Capabilities, and Performance of Low Power Terahertz Sources," *Terahertz Science and Technology, IEEE Transactions on*, vol. 1, no. 1, pp. 33–53, 2011.
- [19] M. S. Vitiello and A. Tredicucci, "Tunable Emission in THz Quantum Cascade Lasers," *Terahertz Science and Technology, IEEE Transactions on*, vol. 1, no. 1, pp. 76–84.
- [20] J. Federici and L. Moeller, "Review of terahertz and subterahertz wireless communications," *Journal of Applied Physics*, vol. 107, no. 11, pp. 111101–111101–22, 2010.
- [21] T. Idehara, T. Saito, I. Ogawa, and Y. Tatematsu, "High power THz technologies opened by high power radiation sources - gyrotrons," *2010 International Kharkov Symposium on Physics and Engineering of Microwaves, Millimeter and Submillimeter Waves (MSMW)*, 2010.

-
- [22] A. Brown, K. Brown, J. Chen, K. Hwang, N. Koliass, and R. Scott, "W-band GaN power amplifier MMICs," *Microwave Symposium Digest (MTT), 2011 IEEE MTT-S International*, pp. 1–4, 2011.
- [23] M. Micovic, A. Kurdoghlian, A. Margomenos, D. F. Brown, K. Shinohara, S. Burnham, I. Milosavljevic, R. Bowen, A. J. Williams, P. Hashimoto, R. Grabar, C. Butler, A. Schmitz, P. Willadsen, and D. Chow, "92-96 GHz GaN power amplifiers," in *2012 IEEE/MTT-S International Microwave Symposium - MTT 2012*, pp. 1–3, IEEE, 2012.
- [24] J. Schellenberg, E. Watkins, M. Micovic, B. Kim, and K. Han, "W-band, 5W solid-state power amplifier/combiner," *2010 IEEE MTT-S International Microwave Symposium Digest (MTT)*, pp. 240–243, 2010.
- [25] L. A. Samoska, "An Overview of Solid-State Integrated Circuit Amplifiers in the Submillimeter-Wave and THz Regime," *IEEE Transactions on Terahertz Science and Technology*, vol. 1, no. 1, pp. 9–24.
- [26] D. Pardo, J. Grajal, C. G. Perez-Moreno, and S. Perez, "An Assessment of Available Models for the Design of Schottky-Based Multipliers Up to THz Frequencies," *Terahertz Science and Technology, IEEE Transactions on*, vol. 4, no. 2, pp. 277–287, 2014.
- [27] P. Kirby, Y. Li, Q. Xiao, J. L. Hesler, and J. Papapolymerou, "Power combining multiplier using HBV diodes at 260 GHz," in *Microwave Conference, 2008. APMC 2008. Asia-Pacific*, pp. 1–4, IEEE, 2008.
- [28] J. V. Siles, B. Thomas, and G. Chattopadhyay, "Design of a high-power 1.6 THz Schottky tripler using 'on-chip' power-combining and Silicon micromachining," *Proceedings of 22 nd International Symposium on Space Terahertz Technology, Tucson.*, 2011.
- [29] J. V. Siles and Maestrini, "A Single-Waveguide In-Phase Power-Combined Frequency Doubler at 190 GHz," *Microwave and Wireless Components Letters*, vol. 21, no. 6, pp. 332–334, 2011.
- [30] A. Maestrini, J. Ward, J. Gill, C. Lee, B. Thomas, R. Lin, G. Chattopadhyay, and I. Mehdi, "A Frequency-Multiplied Source With More Than 1 mW of Power Across the 840-900-GHz Band," *Microwave Theory and Techniques, IEEE Transactions on*, vol. 58, no. 7, pp. 1925–1932, 2010.
- [31] M. P. DeLisio and R. York, "Quasi-optical and spatial power combining," *IEEE Transactions on Microwave Theory and Techniques*, vol. 50, pp. 929–936, Mar. 2002.

- [32] W. Lam, H. Chen, D. Rutledge, C. Jou, and N. Luchmann, "Diode-grids for millimeter-wave phase-shifters and frequency doublers," *Antennas and Propagation Society International Symposium, 1987*, vol. 25, pp. 1190–1193, 1987.
- [33] R. M. Weikle II, D. S. Kurtz, and R. F. Bradley, "A Ku-band diode-array frequency tripler," in *IEEE Antennas and Propagation Society International Symposium 1997. Digest (Cat. No.97CH36122)*, (New York, NY, USA), pp. 2456–9, Sch. of Eng. Appl. Sci., Virginia Univ., Charlottesville, VA, USA, IEEE, 1997.
- [34] D. Steup, A. Simon, M. Shaalan, A. Grüb, and C. I. Lin, "A quasioptical doubler-array," *International Journal of Infrared and Millimeter Waves*, vol. 17, no. 5, pp. 843–856, 1996.
- [35] R. J. Hwu, C. F. Jou, W. W. Lam, U. Lieneweg, D. C. Streit, N. C. Luhmann, J. Maserjian, and D. B. Rutledge, "Watt-level millimeter-wave monolithic diode-grid frequency multipliers," *Microwave Symposium Digest, 1988., IEEE MTT-S International*.
- [36] A. Moussessian, M. Wanke, Y. Li, J.-C. Chiao, J. Allen, T. Crowe, and D. Rutledge, "A terahertz grid frequency doubler," *Microwave Theory and Techniques, IEEE Transactions on*, vol. 46, no. 11, pp. 1976–1981, 1998.
- [37] R. J. Hwu, C. F. Jou, N. C. Luhmann, M. Kim, W. W. Lam, Z. B. Popovic, and D. B. Rutledge, "Array concepts for solid-state and vacuum microelectronics millimeter-wave generation," *IEEE Transactions on Electron Devices*, vol. 36, no. 11, pp. 2645–2650, 1989.
- [38] N. Paravastu and R. M. Weikle II, "A 40-80 GHz quasi-optical balanced doubler using nested ring-slot antennas," *Antennas and Propagation Society International Symposium, 2002. IEEE*, pp. 1–4, Feb. 2004.
- [39] J. Stake, S. Hollung, L. Dillner, and E. Kollberg, "A 141-GHz integrated quasi-optical slot antenna tripler," *Antennas and Propagation Society International Symposium, 1999. IEEE*, vol. 4, pp. 2394–2397 vol.4, 1999.
- [40] S. Hollung, J. Stake, L. Dillner, M. Ingvarson, and E. Kollberg, "A distributed heterostructure barrier varactor frequency tripler," *IEEE Microw. Guid. Wave Lett. (USA)*, vol. 10, pp. 24–26, Jan. 2000.
- [41] J. B. Hacker, A. L. Sailer, B. Brar, G. Nagy, R. L. J. Pierson, and J. A. Higgins, "A high-power W-band quasi-optical frequency tripler," *2003 IEEE MTT-S International Microwave Symposium Digest*, vol. 3, pp. 1859–1862, 2003.
- [42] S. A. Rosenau, *Quasi-optical overmoded waveguide frequency multiplier grid arrays*. PhD thesis, University of California Davis, 2001.

-
- [43] D. B. Rutledge, N. S. Cheng, R. York, R. M. Weikle II, and M. P. De Lisio, "Failures in power-combining arrays," *IEEE Trans. Microw. Theory Tech.*, vol. 47, pp. 1077–1082, July 1999.
- [44] P. Penfield and R. P. Rafuse, *Varactor Applications*. MIT Press, 1962.
- [45] E. Kollberg and A. Rydberg, "Quantum-Barrier-Varactor Diodes for High-Efficiency Millimeter-Wave Multipliers," *Electronics Letters*, vol. 25, no. 25, pp. 1696–1698, 1989.
- [46] J. M. Manley and H. E. Rowe, "Some General Properties of Nonlinear Elements—Part I. General Energy Relations," in *Proceedings of the IRE*, pp. 904–913, 1956.
- [47] C. H. PAGE, "Frequency Conversion with Positive Nonlinear Resistors," *Journal of Research of the National Bureau of Standards*, vol. 56, no. 4, pp. 179–182, 1956.
- [48] A. Uhler, "The Potential of Semiconductor Diodes in High-Frequency Communications," in *Proceedings of the IRE*, pp. 1099–1115, 1958.
- [49] K. Krishnamurthi and R. G. Harrison, "Analysis of symmetric-varactor-frequency triplers," *Microwave Symposium Digest, 1993., IEEE MTT-S International*, pp. 649–652, 1993.
- [50] J. Stake, S. H. Jones, L. Dillner, S. Hollung, and E. L. Kollberg, "Heterostructure-barrier-varactor design," *Microwave Theory and Techniques, IEEE Transactions on*, vol. 48, no. 4, pp. 677–682, 2000.
- [51] L. Dillner, J. Stake, and E. L. Kollberg, "Analysis of symmetric varactor frequency multipliers," *Microwave And Optical Technology Letters*, vol. 15, pp. 26–29, May 1997.
- [52] E. L. Kollberg, T. J. Tolmunen, M. A. Frerking, and J. R. East, "Current Saturation in Submillimeter Wave Varactors," *IEEE Trans. Microw. Theory Tech.*, vol. 40, pp. 831–838, May 1992.
- [53] J. Stake, L. Dillner, S. H. Jones, C. Mann, J. Thornton, J. R. Jones, W. L. Bishop, and E. Kollberg, "Effects of self-heating on planar heterostructure barrier varactor diodes," *IEEE Trans. Electron Devices (USA)*, vol. 45, pp. 2298–2303, Nov. 1998.
- [54] B. Diamond, "Idler Circuits in Varactor Frequency Multipliers," *IEEE Transactions on Circuit Theory*, vol. 10, pp. 35–44, Mar. 1963.
- [55] Z. B. Popovic, R. M. Weikle II, M. Kim, and D. B. Rutledge, "A 100-MESFET planar grid oscillator," *Microwave Theory and Techniques, IEEE Transactions on*, vol. 39, no. 2, pp. 193–200, 1991.

- [56] R. M. Weikle II, *Quasi-optical planar grids for microwave and millimeter-wave power combining*. PhD thesis, California Institute of Technology, 1992.
- [57] R. Eisenhart and P. Khan, "Theoretical and Experimental Analysis of a Waveguide Mounting Structure," *Microwave Theory and Techniques, IEEE Transactions on*, vol. 19, no. 8, pp. 706–719, 1971.
- [58] W. Shiroma, S. Bundy, S. Hollung, B. Bauernfeind, and Z. Popovic, "Cascaded active and passive quasi-optical grids," *Microwave Theory and Techniques, IEEE Transactions on*, 1995.
- [59] D. S. Kurtz, R. M. Weikle II, and R. F. Bradley, "A Ku-band diode-array frequency tripler," *Antennas and Propagation Society International Symposium, 1997. IEEE., 1997 Digest*.
- [60] X. Qin, C. Domier, N. C. Luhmann, H. X. L. Liu, E. Chung, L. Sjogren, and W. Wu, "Millimeter-wave monolithic barrier n-n+ diode grid frequency doubler," *Applied Physics Letters*, vol. 62, no. 14, p. 1650, 1993.
- [61] C. F. Jou, W. W. Lam, H. Z. Chen, K. S. Stolt, N. C. Luhmann, and D. B. Rutledge, "Millimeter-Wave Diode-Grid Frequency Doubler," *IEEE Trans. Microw. Theory Tech.*, vol. 36, pp. 1507–1514, Nov. 1988.
- [62] J. Stake, L. Dillner, and E. L. Kollberg, "Heterostructure barrier varactors on copper substrate," *Electronics Letters*, vol. 35, no. 4, pp. 339–341, 1999.
- [63] P. Goldsmith, *Quasioptical Systems: Gaussian Beam Quasioptical Propagation and Applications*. Wiley-IEEE Press, 1997.
- [64] J. Vukusic, T. Bryllert, T. Arezoo Emadi, M. Sadeghi, and J. Stake, "A 0.2-W Heterostructure Barrier Varactor Frequency Tripler at 113 GHz," *Electron Device Letters, IEEE*, vol. 28, pp. 340–342, May 2007.
- [65] P. Siegel, "Terahertz technology in biology and medicine," *IEEE Transactions on Microwave Theory and Techniques*, vol. 52, no. 10, pp. 2438–2447, 2004.
- [66] V. Wallace, A. Fitzgerald, and E. Pickwell, "Terahertz pulsed spectroscopy of human basal cell carcinoma," *Applied spectroscopy*, Jan. 2006.
- [67] Z. Taylor, R. Singh, M. Culjat, J. Suen, W. Grundfest, H. Lee, and E. Brown, "Reflective terahertz imaging of porcine skin burns," *Optics Letters*, vol. 33, no. 11, pp. 1258–1260, 2008.
- [68] J.-H. Son, "Terahertz electromagnetic interactions with biological matter and their applications," *Journal of Applied Physics*, vol. 105, no. 10, p. 102033, 2009.

-
- [69] V. P. Wallace and A. J. Fitzgerald, “Terahertz pulsed imaging of human breast tumors,” *Radiology*, vol. 239, pp. 533–540, Apr. 2006.
- [70] E. Pickwell, B. E. Cole, A. J. Fitzgerald, M. Pepper, and V. P. Wallace, “In vivo study of human skin using pulsed terahertz radiation,” *Physics in Medicine and Biology*, vol. 49, pp. 1595–1607, Apr. 2004.
- [71] H. Hoshina, A. Hayashi, N. Miyoshi, F. Miyamaru, and C. Otani, “Terahertz pulsed imaging of frozen biological tissues,” *Applied Physics Letters*, vol. 94, p. 123901, Jan. 2009.
- [72] A. Fitzgerald, E. Berry, N. Zinov’ev, S. Homer-Vanniasinkam, R. Miles, J. Chamberlain, and M. Smith, “Catalogue of human tissue optical properties at terahertz frequencies,” *Journal of Biological Physics*, vol. 29, no. 2, pp. 123–128, 2003.
- [73] K. Cooper, R. Dengler, G. Chattopadhyay, E. Schlecht, J. Gill, A. Skalare, I. Mehdi, and P. Siegel, “A high-resolution imaging radar at 580 GHz,” *IEEE Microwave and Wireless Components Letters*, vol. 18, no. 1, pp. 64–66, 2008.
- [74] M. A. Morgan and S. Pan, “Graphical Prediction of Trapped Mode Resonances in Sub-mm and THz Waveguide Networks,” *Terahertz Science and Technology, IEEE Transactions on*, vol. 3, no. 1, pp. 72–80, 2013.
- [75] C.-T. Cheung, J. Hacker, G. Nagy, and D. Rutledge, “A waveguide mode-converter feed for a 5-W, 34-GHz grid amplifier,” *Microwave Symposium Digest, 2002 IEEE MTT-S International*, vol. 3, pp. 1523–1526, 2002.